JMEPEG (2012) 21:2044–2052
DOI: 10.1007/s11665-012-0163-x

1059-9495/$19.00

An Analytical Model for Evaluation of Bending Angle in Laser Forming of Metal Sheets

Francesco Lambiase

(Submitted May 24, 2011; in revised form January 18, 2012)

In this study, an analytical model is developed to evaluate the bending angle in laser forming of metal sheets. The model is based on the assumption of elastic-bending theory without taking into account plastic deformation during heating and cooling phases. A thermal field is first established, then the thermal component of deformation is calculated and it is used in the strain balance to evaluate the bending angle. The basic idea is that it is possible to use a two-layer model whereas the heated layer thickness depends on the effective temperature distribution along the sheet thickness. A comprehensive experimental study is carried out and the main process parameters, i.e., laser power, scanning speed, sheet thickness, were varied among several levels to evaluate the accuracy of the developed model. Model predictions were confirmed by experimental measurements especially on materials with low conductivity. The established analytical model has demonstrated to provide a great insight into the process parameters effects onto the deformation mechanism within pure temperature gradient mechanism and bucking to temperature gradient transition conditions.

Keywords analytical model, bending mechanism, laser forming

1. Introduction

Laser-forming process consists in heating a sheet (or tube) surface by means of a laser beam generating a thermal stress which in turn produces sheet bending. Three main deformation mechanisms have been established for laser bending namely, temperature gradient mechanism (TGM), buckling mechanism (BM), and upsetting mechanism (UM) (Ref 1). The TGM implies a rapid heating of metallic substrates with consequent low heat conduction into thickness direction. A steep thermal gradient originates within the material, thereby producing a differential thermal expansion and plastic deformation through thickness. In BM, there is an almost uniform temperature distribution along thickness and bending can be either toward or away from laser beam depending on process conditions. In UM, a substrate is compressed with an almost constant strain through thickness, causing localized shortening and an increase of local thickness (Ref 2). The transition from one to another mechanisms is not sharp and depends on the thermal profile occurring along sheet thickness direction and ultimately by the characteristics of laser beam dimension, material properties, and sheet thickness. Particularly, TGM is dominant under conditions corresponding to a small modified Fourier number $F_0 = \alpha \cdot l/(s^2 \cdot v)$ (Ref 3, 4). Many studies have been aimed at analyzing laser bending deformation mechanism based on experimental analysis (Ref 5, 6), analytical modeling (Ref 7-10), and finite element modeling (Ref 11-14). Both finite element models and some analytical models, mainly those involving numerical solution (Ref 7), allow to evaluate the final sheet shape with great accuracy (such models can also provide information on deviation of bending angle from mean value along the scanning direction, side effects, stress and strain distributions, and accurate temperature fields). The precision of these models is further improved by the possibility to involve temperature-dependent mechanical and physical characteristics of material, temperature, and stress fields during heating and cooling phases. However, FEM models are affected by large computational effort and long calculation time (each

Francesco Lambiase, Department of Mechanical Energy and Management Engineering, University of L'Aquila, Monteluco di Roio, 67040 l'Aquila, AQ, Italy. Contact e-mail: francesco.lambiase@univaq.it.

Nomenclature

α	Thermal diffusivity
α_b	Final bending angle
α_{th}	Coefficient of thermal expansion
ρ	Material density
A	Absorption coefficient
B	Sheet width (orthogonal to scanning direction)
E	Young modulus
K	Curvature
L	Sheet length (along scanning direction)
P	Laser power
T	Temperature
T_0	Room temperature
T_{up}	Temperature of irradiated surface
c_p	Heat capacity
d	Laser beam length (along scanning direction)
k	Coefficient of thermal conductivity
l	Laser beam width (orthogonal to scanning direction)
q	Absorbed power
s	Sheet thickness
s_1	Thickness of heated volume
t	Interaction time
v	Laser scanning velocity

FEM simulation takes more than an hour on a powerful computer) which limits their use during early design phase and process optimization. Analytical models with numerical solution are also affected by significant computational time especially for evaluation of thermal field even though they require less computational time (almost some minutes) (Ref 8, 15). In addition, as previously mentioned, highly accurate predictions are achieved when a detailed knowledge of temperature-dependent mechanical and physical properties of material are involved within the model. On the contrary, closed-form analytical models (Ref 5, 9, 10) assume constant values of mechanical and thermal material behavior and are they based on some simplifications which allow to determine bending angle in few instants. Since the pioneer model developed by Vollertsen (Ref 5) based on elastic-bending theory, some more models have been proposed: Yau and Chan (Ref 9) introduced the effect of counter bending during heating and cooling, Kyrsanidi et al. (Ref 15) considered plastic bending during heating phase. The main limit of such models is represented by a poor accuracy especially at low scanning speeds. At this process conditions a co-existence of BM and TGM occurs and bending angle trend versus scanning velocity shows a peak.

The aim of this study is to develop an analytical model capable to evaluate the bending angle in laser forming not only under pure TGM but also under co-existing BM and TGM. Particularly, an analytical model is proposed and a campaign of experiments is conducted to evaluate the accuracy of such a model. A diode laser with rectangular spot is used and the effects of main process parameters, i.e., laser power, scanning speed, and sheet thickness are varied among several levels. In addition, some data reported in literature are also taken into account to verify the model accuracy over a wider range of process conditions and materials. Finally, conclusions are drawn on analytical and experimental findings.

1.1 Analytical Model

In laser bending, high gradients of temperature are generated; therefore, during the process stress-induced strain occur. During heating phase, a sheet bends away from laser beam because of thermal expansion of irradiated surface; while, on the other hand, the sheet undergoes an opposite bending during cooling phase because of contraction of irradiated surface. During heating and cooling phases stress arise along sheet thickness determining sheet bending; however, stress generated during cooling phase is significantly smaller than that occurring during heating. Different approaches have been adopted to determine the effect of process parameters on bending angle analytically. In the present model, a two-layer model is assumed to determine the thermal strain and in turn the bending angle. The attempt is to overcome the limits of Vollertsen model (Ref 5) to accurately account the bending angle for process conditions involving gentile temperature gradients along the sheet thickness especially under low scanning velocities. Such difficulty stated in the assumption that the heated layer thickness does not depends on effective temperature distribution along sheet thickness. The proposed model is based on the evaluation of thermal strain generated by laser heat flux (that is calculated with an energy balance) and successively, the thermal strain is used to compute the bending angle with strain balance and assuming a plane strain condition. Since the model is based on elastic theory bending as Vollertsen model, such model hypothesis are summarized as follows:

1. the heat loss due to convection, radiation with surrounding environment, and conduction with material surrounding the scanning path are neglected;
2. the thermal strain can be computed supposing that the total heat absorbed by the material concentrates within the upper volume of thickness s_1;
3. regardless the process conditions, the heated volume thickness is half of the sheet thickness;
4. the strain balance allows the calculation of bending angle;
5. the deformation is uniform along scanning path direction.

Although the previously mentioned assumptions extremely simplify the laser heating process, a good agreement with experimental results was found for several materials and process conditions. However, it is observed that, Vollertsen model does not provide accurate predictions of bending angle at small scanning speeds (Ref 5). Indeed, under given conditions the bending angle can show a peak (indicating a prevalent BM deformation mode) then it decreases (because of transition to TGM) with scanning velocity, while, on the other hand, previous models (Ref 5, 9, 10) predict a monotonic decrease of bending angle with scanning velocity. This is due to a poor temperature gradient along sheet thickness. Among the others, an excessive simplification formulated by Vollertsen is the independency of heated volume thickness by process parameters. Such hypothesis is in clear contrast with both theoretical prediction and experimental findings on temperature profile along thickness direction. Indeed, the temperature gradient mainly depends on scanning speed velocity and sheet thickness other than material characteristics, laser power, and spot size. Therefore, in the present model, the heated volume thickness s_1 depends on the temperature profile generated at given process conditions, sheet thickness, and material characteristics, as shown in Fig. 1. According to elastic-bending theory, Vollertsen estimated the bending angle for $s_1 \neq s/2$ as reported in Eq 1:

$$\begin{cases} \alpha_B = \frac{l \cdot L(s-s_1) \cdot s_1 \cdot T \cdot \alpha_{th}}{I} \\ I = \frac{1}{12} L s^3 + \left(\frac{s}{2} - s_1\right)^2 L s \end{cases} \quad \text{(Eq 1)}$$

Considering that the increase of temperature ΔT of heated volume is given by the external laser heat flux which

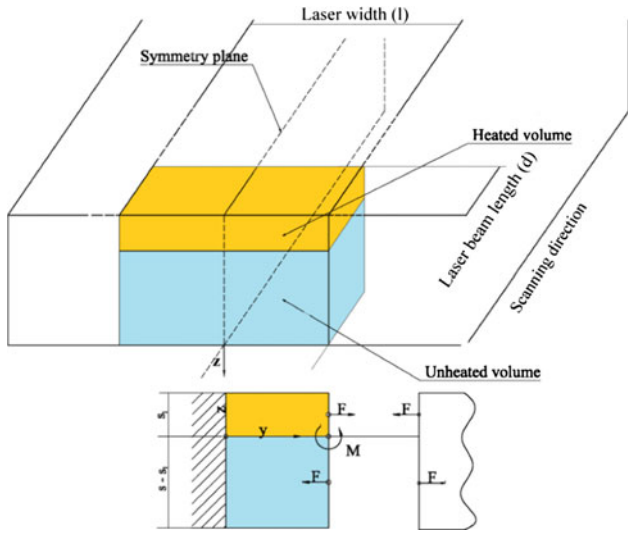

Fig. 1 Representation of two-layer model with variable heated volume thickness

concentrates within the heated volume, ΔT and α_B can be calculated by Eq 2 and 3, respectively.

$$\Delta T = \frac{A \cdot P}{(l \cdot d \cdot s_1)} \cdot \frac{d}{v} \cdot \frac{1}{\rho \cdot c_p} = \frac{A \cdot P}{(l \cdot s_1) \cdot v \cdot \rho \cdot c_p} \quad \text{(Eq 2)}$$

$$\alpha_B = \frac{3AP(s - s_1)\alpha_{th}}{s(s^2 - 3s \cdot s_1 + 3s_1) \cdot \rho v c_p} \quad \text{(Eq 3)}$$

1.2 Evaluation of Heated Volume Thickness, s_1

An approximation of heated volume thickness can be achieved considering the thermal profile along thickness direction generated by given treatment conditions and material. Neglecting the heat loss due to conduction during heating phase, a mono-dimensional heat conduction is established along sheet thickness. Therefore, the temperature distribution can be calculated as in Eq 4 (Ref 15):

$$T(z) = T_0 + T_{up} e^{-\left(\frac{\rho c v}{2k} z\right)} \quad \text{(Eq 4)}$$

To obtain a sound value of T_{up}, it may refer to the internal energy distribution ΔU along sheet thickness that is given by Eq 5 (whereas the thermal characteristics of material are constant):

$$\Delta U = \int_0^Q dQ = \rho c d l \int_0^s T(z)\, dz \quad \text{(Eq 5)}$$

Therefore, substituting the Eq 4 in 5:

$$Q = \frac{2d\left(1 - e^{-\frac{s v \rho c}{2k}}\right)}{v} k l T_{up}$$

In addition, since the internal energy is changed due to laser heating:

$$Q = APt = AP\frac{d}{v} \quad \text{(Eq 6)}$$

Therefore

$$T(z) = T_{up} e^{-\left(\frac{\rho c v}{2k} z\right)} = \frac{e^{\frac{v \rho c v}{2k}} PA}{2\left(-1 + e^{\frac{v \rho c}{2k}}\right) kl} e^{-\left(\frac{\rho c v}{2k} z\right)} = \frac{AP}{2kl\left[1 - \exp\left(-\frac{\rho v c}{2k}\right)\right]} \exp\left(-\frac{\rho v c}{2k} z\right) \quad \text{(Eq 7)}$$

The assumption made in the present model is that the heated volume is that on which a given portion of external heating energy, say γ, concentrates on that volume, therefore, s_1 is such that it satisfies Eq 8.

$$\int_0^{\gamma Q} dQ = \int_0^{s_1} \rho c d l T(z)\, dz \quad \text{(Eq 8)}$$

$$\gamma Q = \gamma AP\frac{d}{v} = \frac{2d\left(1 - e^{-\frac{s_1 \rho c}{2k}}\right) k l T_{up}}{v}$$

Therefore

$$s_1 = 1 - \frac{2k \mathrm{Log}\left[-e^{\frac{v \rho c}{2k}}(-1 + \gamma) + \gamma\right]}{v \rho c} \quad \text{(Eq 9)}$$

As can be observed, the heated volume thickness, s_1, depends on material characteristics and scanning velocity other than the γ parameter, while, on the other hand it does not depend on the laser power. Figure 2 depicts schematically the temperature-dependent two-layer assumptions. Indeed, the temperature distribution along thickness direction drops exponentially and all the heat absorbed by laser radiation, Q, is used to heat up the volume under laser beam. The model assumes that only a portion of sheet thickness s_1 undergoes compressive stress during heating (yellow portion in Fig 2b) while the remaining $s - s_1$ remains at initial temperature (blue portion). Finally, an equivalent uniform temperature distribution is assumed within the heated volume as depicted in Fig. 2c thus the thermal stress and strain fields can be calculated by the above equations. The developed model was validated against a series of experimental tests and some data reported in literature (Ref 15). In latter case, the spot size is 32 mm and laser power ranges between 1 and 3 kW. The characteristics of materials investigated in Ref 15 are reported in Table 1.

2. Experiments

Laser bending process was carried out on AISI 304 stainless steel, whose thermal properties (Ref 7) are reported in Table 1. Each experiment consisted of two steps: (i) surface laser treatment with a single scan and (ii) measurement of bending angle after the sheet temperature had dropped at room

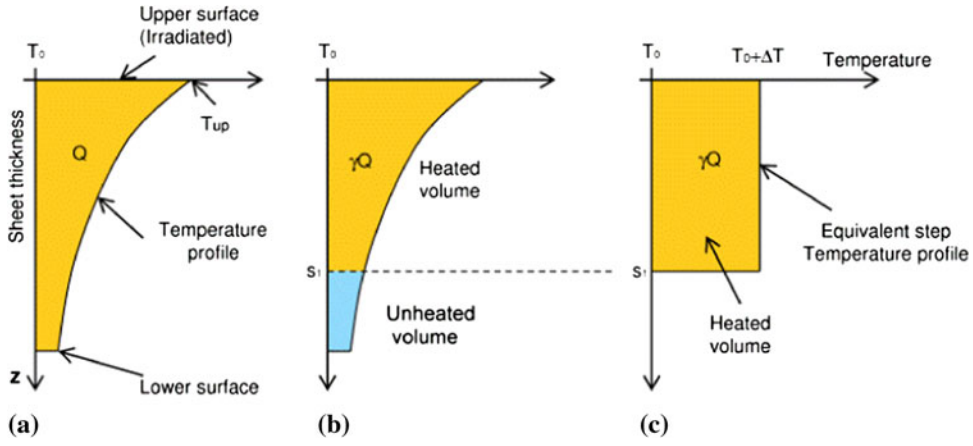

Fig. 2 Schematic representation of temperature distribution along sheet thickness and equivalent step temperature profile (Color figure online)

temperature. The samples are cut by a CO_2 laser to avoid excessive residual stress and distortions prior of laser bending; nevertheless, to ensure a good planarity, the samples curvature was measured before the laser treatment. Any surface coating was realized on sheets to better replicate real industrial conditions. A schematic representation of laser bending equipment is reported in Fig. 3. The sheet is fastened in the short edge (40 mm) and a straight laser scan is performed from one side to the opposite in the middle of the long edge (80 mm). 1 and 2 mm thick samples were tested; therefore, the width to thickness ratios (b/s) were 40 and 20, respectively, which were larger than the critical value 10 which guarantees to avoid the effect of width on final bending angle (Ref 5). A diode laser with a maximum output power of 1,055 kW, over a minimum spot size of 3.6×0.8 mm is used. The scanning speed was varied between 15 and 50 mm/s while the focal position is not varied among the experiments. A series of preliminary tests were carried out to identify the proper technological window which escapes an excessive surface oxidation and melting (because of very low scanning velocity), thus the maximum laser power 550 W was adopted. For each processing condition two replications were carried out to evaluate the variability of the treatment and three measurements of each sample were carried out to estimate the measurements system repeatability. The final sample geometry was measured by means of a laboratory CMM constituted by a numerically controlled table which moved the sample under a short range laser sensor (26-34 mm with nominal repeatability 6 μm) acquiring the z-position.

Table 1 Data of materials investigated

Material	AISI 304	D36	AA 6013
Density, kg/m^3	7850	7860	2700
Specific heat, J/kg · K	500	427	880
Thermal expansion (10-6/K)	17	12	25
Thermal conductivity, W/mK	19	35.1	172
Absorption coefficient	0.42	0.3	0.2

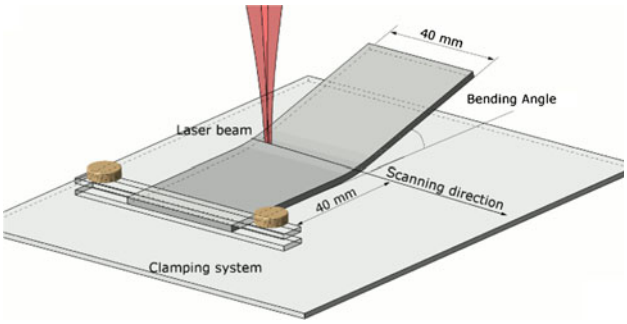

Fig. 3 Schematic illustration of straight line laser bending process

3. Results and Discussion

Before dealing with discussion on model results, a brief analysis of experimental results, experiments variability, and

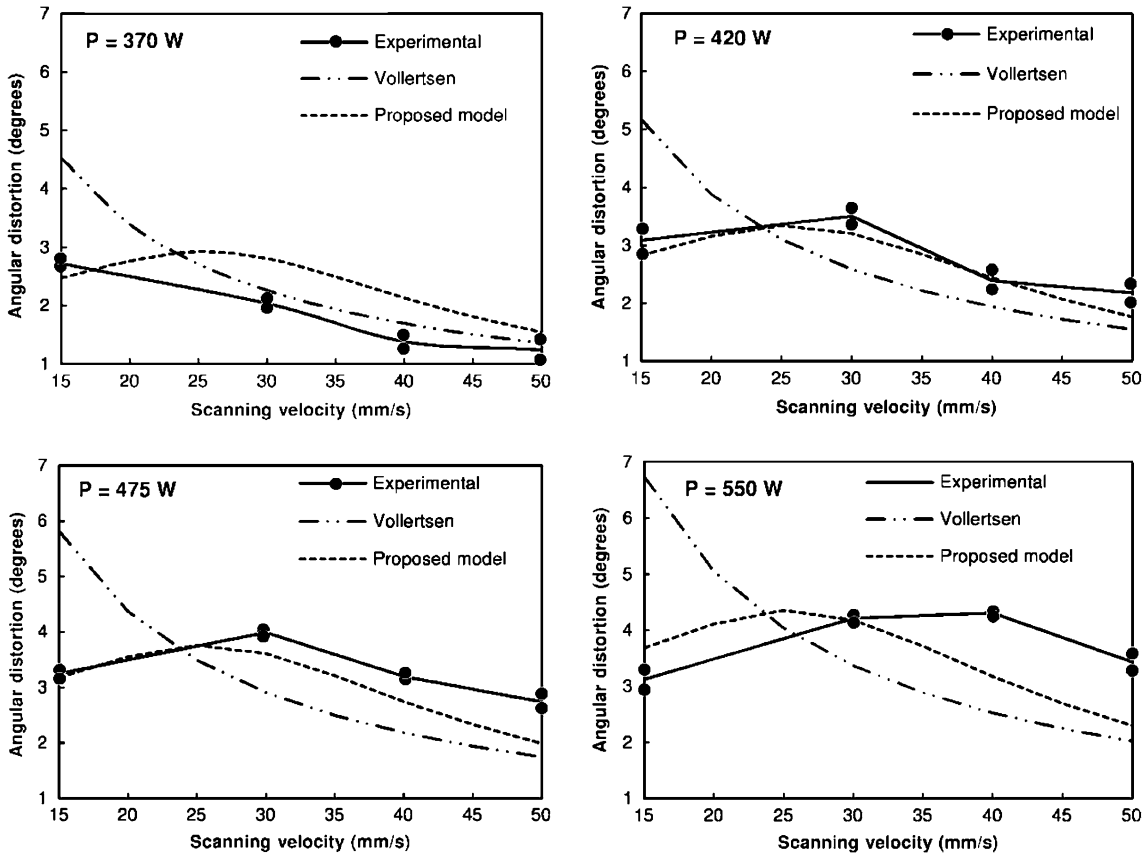

Fig. 4 Experimental measurement and models predictions of angular distortion under different process conditions on sample of thickness of s = 1 mm (material AISI 304)

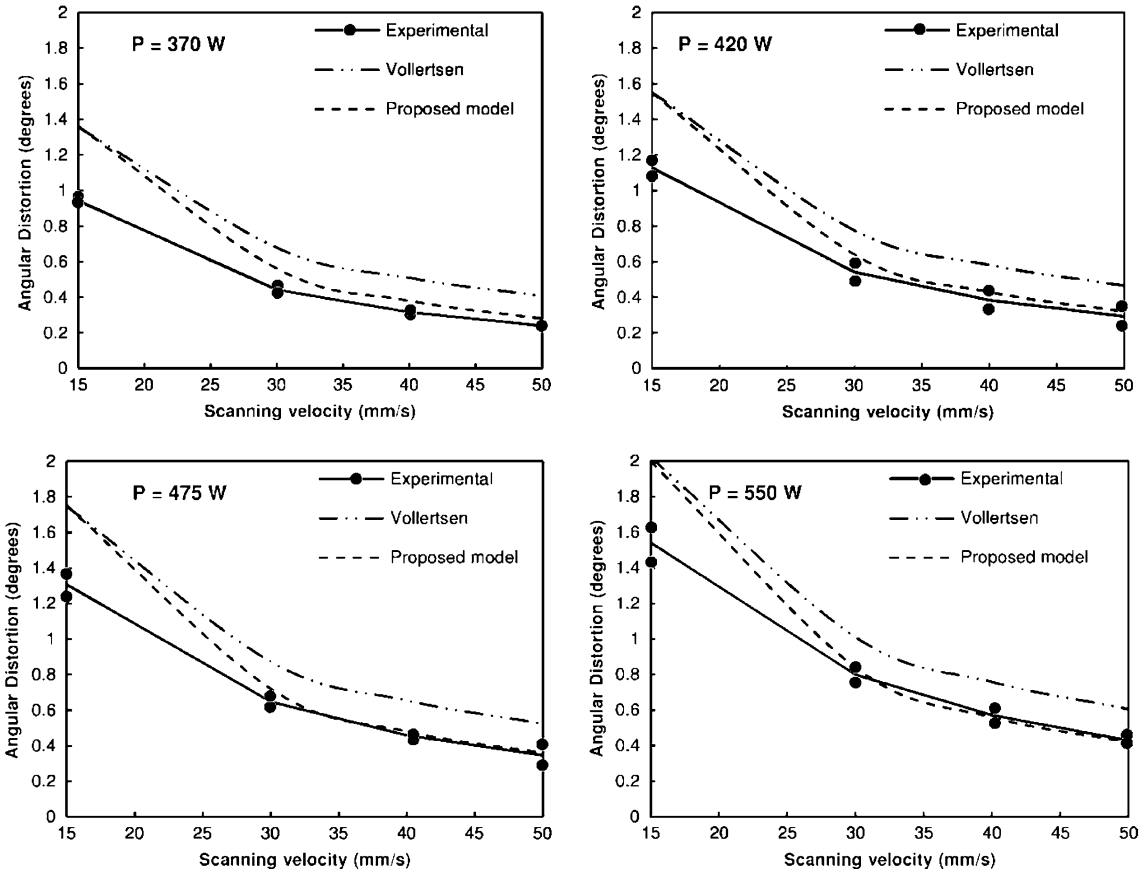

Fig. 5 Experimental measurement and models predictions of angular distortion under different process conditions on sample of thickness of $s = 2$ mm (material AISI 304)

measuring system repeatability is reported. Regardless the process conditions, the three repetitions of bending angle measurements on each sample provided a maximum deviation of 0.02° thus ensuring a good repeatability of measurement system since it was more than one order of magnitude smaller than the minimum measured bending angle ($\alpha = 0.3°$ for $P = 370$ W, $v = 50$ mm/s, $s = 2$ mm). Such a small value was obtained by maximizing the distance of measuring points in transverse direction (perpendicular to scanning-longitudinal direction) that was of 30 mm.

Concerning the repetitions of laser bending tests, an overall low variability was observed regardless the processing conditions, the average divergence between repetitions being lower than 5% and the maximum divergence being smaller than 20%.

3.1 Model Validation

As above mentioned, the proposed model accuracy was evaluated by a comparison of model predictions with experimental measurements performed on different materials: a stainless steel AISI 304 and a shipbuilding steel D36. The testing conditions such as scanning velocity, laser power, and sample thickness are summarized in Table 2. As can be observed the experimental conditions occurring in the developed experimental tests and those conducted in Ref 15 are extremely heterogeneous in terms of laser power range, beam size, irradiance scanning velocity, and sample thickness. However, the energy flux range calculated as the product of interaction time by irradiance is similar. In order to employ the developed model, the γ parameter is found by regression of experimental data at different process conditions and $\gamma = 0.85$ is assumed. Therefore, the heated volume thickness is such that the 85% of absorbed power concentrates on such a volume.

Table 2 Experimental conditions

Testing conditions	AISI 304	D36
Power, W	370-550	1000-3000
Beam size, mm^2	2.90	1024
Irradiance, W/mm^2	130-190	1-3
Scanning velocity, mm/s	15-50	2-23
Sample thickness, mm	1-2	6
Interaction time, s	0.016-0.05	0.25-2.8
Energy flux, J/mm^2	2.1-9.5	1-34

The proposed model results are compared with the experimental measurements as well as Vollertsen's model under different process conditions and are reported in Fig. 3 to 6. In particular, Fig. 3 shows the bending angles (also referenced as angular distortion) for AISI 304 with sample thickness of 1 mm. As can be observed, at low scanning velocities, the angular distortion shows a peak, which generally occurs at a scanning velocity of 30 mm/s. The occurrence of such a peak depends on laser power, since it does not appear at low power, i.e., 370 W. The presence of a maximum is consistent with the results presented in Ref 15 by Kyrsanidi et al. at lower scanning velocity, i.e., $v = 2.5$ mm/s whereas the process conditions involved a co-existence of bucking mechanism and TGMs.

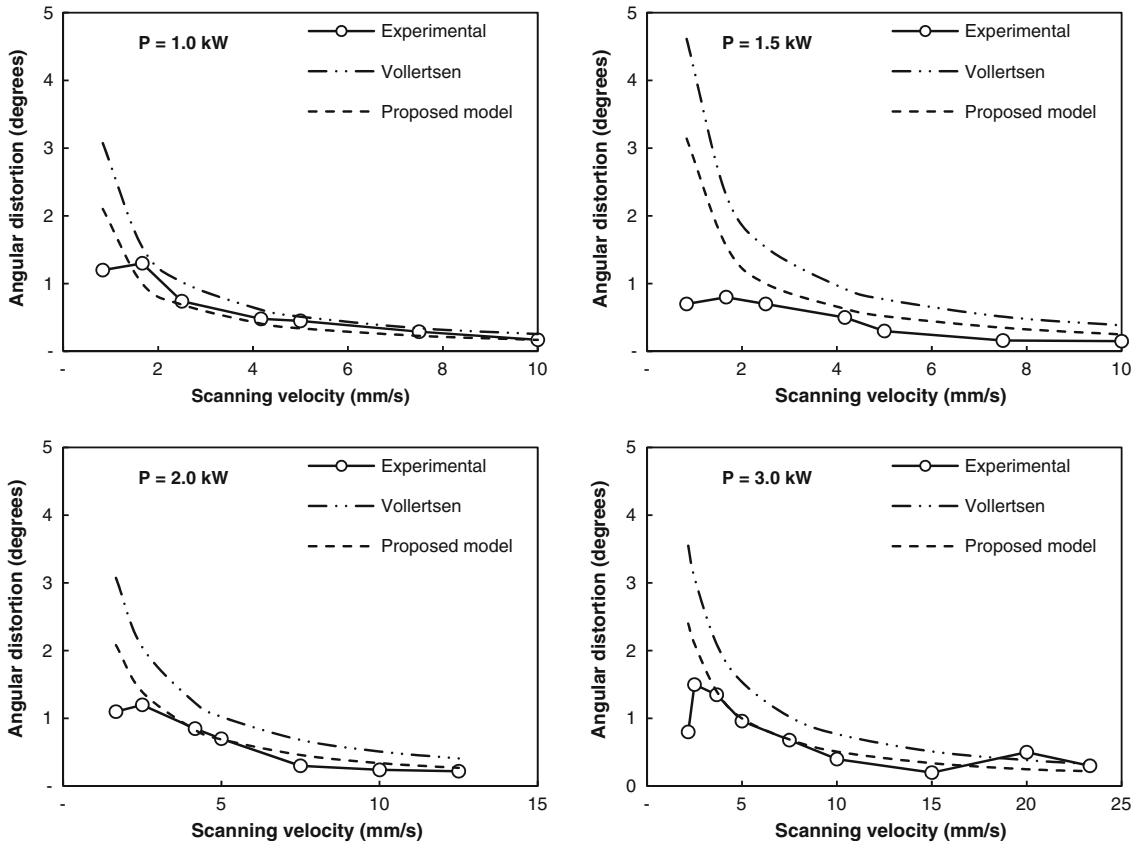

Fig. 6 Experimental measurement and models predictions of angular distortion under different process conditions on sample of thickness of s = 6 mm (D36 steel, Ref 8)

The experimental trends of angular distortion are reported in Fig. 4 with Vollertsen and the proposed model results for sheet thickness of 2 mm. A higher sample thickness involves a different behavior of bending angle with respect to scanning velocity; indeed, regardless the laser power, any peak was observed on samples with thickness of 2 mm. At the lower scanning speed, i.e., v = 15 mm/s, the proposed model predicts the same angular distortion of Vollertsen model, regardless the laser power and both models predict a larger bending angle as compared to the experimental measurements. This discrepancy can be addressed to the simplification of neglecting of thermal conduction towards the surrounding material that is relevant especially at low scanning speeds since a higher interaction time. However, the proposed model predictions yield the experimental findings at higher scanning velocities at all process conditions, demonstrating that the heat conduction under these conditions is negligible. The results of the proposed model are consistent with experimental findings regardless the scanning velocity and sample thickness. On the other hand, Vollertsen model is characterized by large divergence with experimental findings especially under low speeds and thin samples, i.e., s = 1 mm. This is due to the assumption of constant heated volume thickness. Indeed, at small scanning velocities, the thermal gradient is negligible; therefore, the effective heated volume has a thickness significantly larger than the half sample thickness. Thus, even though the greater absorbed energy due to higher interaction time, such an energy spreads over a larger volume causing a smaller increase of temperature. The accuracy of the proposed model is also evaluated by a comparison with experimental results reported in Ref 15. The lower scanning velocity is one order of magnitude lower than that occurring under the above-described experimental test. Also, the transition from BM to TGM can be appreciated as increasing the scanning velocity and a peak of bending angle can be still observed. However, neither Vollertsen model nor the developed model was able to predict such a peak because of the higher heat loss for conduction due to a larger wall thickness and material conductivity. On the other hand, a better correspondence of models results and experimental data are found at higher scanning velocities, the predictions of the proposed model being more accurate with respect to Vollertsen ones.

The experimental measurements, Vollertsen and proposed model predictions on AISI 304 are reported in Fig. 5. Indeed, the slope of linear regression curve of proposed model for the thinner sample is 1.8 and it is much closer to the ideal value of one with respect to that of Vollertsen's model. In addition, there is a smaller dispersion of data around the regression line as compared to Vollertsen data. Under clear TGM conditions and sheet thickness s = 1 mm both models better agree with experimental findings. Indeed, the regression line slopes are much closer to the unity, i.e., 1.27 and 1.18 for Vollertsen and proposed model, respectively; in addition, data dispersion is sensibly reduced and the mean square error R^2 are 0.98 and 0.99, respectively (Fig. 7).

3.2 Effects of Laser-Forming Parameters

3.2.1 Temperature Field. Figure 8 depicts the temperature distribution along the sheet thickness as predicted by the current model under different scanning speeds. As van be

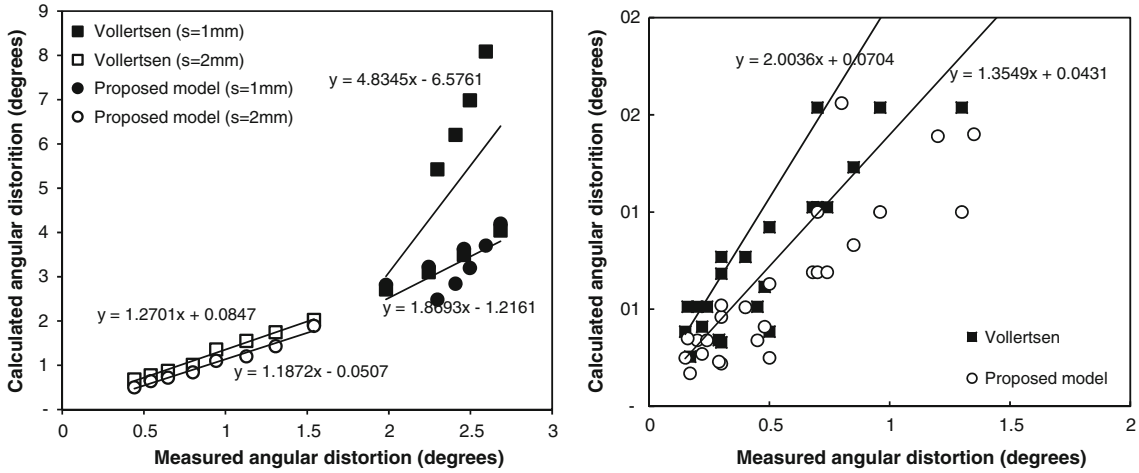

Fig. 7 Comparison of Vollertsen and proposed model predictions with experimental measurements under processing conditions, sample thickness, and materials. (a) AISI 304, (b) D36 (Ref 8)

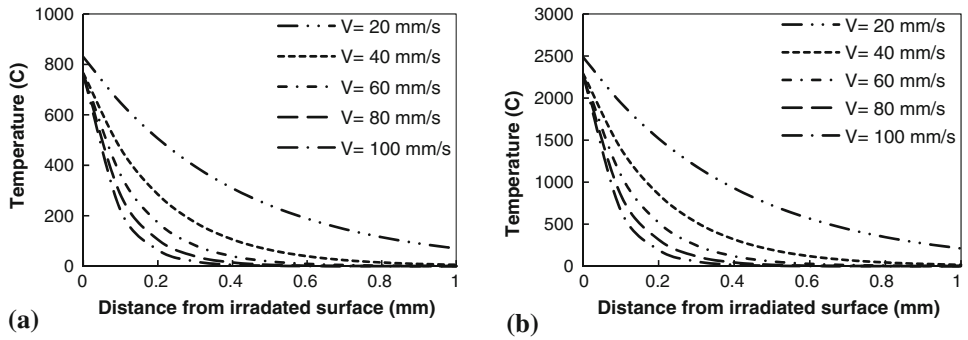

Fig. 8 Temperature distribution as predicted by present model along sheet thickness (s = 1 mm) under different laser powers. (a) P = 250 W, (b) P = 750 W at different scanning velocities

observed, the temperature gradient along sheet thickness direction does not depend on the laser power (from which depends the surface temperature) but it is more affected by scanning speed and material characteristics. Indeed, since the heated volume thickness s_1 only depends on temperature gradient (and not on the absolute values of temperature along thickness), the value of s_1 is not affected by the incident laser power but rather by the scanning speed. As expected, the higher the scanning speed, the higher the temperature gradient along the sheet thickness and the lower the heated volume thickness s_1. Therefore a higher increase of temperature ΔT occurs on the heated volume. On the other hand, the higher the scanning speed involves a lower interaction time and then a lower energy can be absorbed by the sheet. These opposite phenomena determines the occurrence of the peak of bending angle for low scanning speed in the transition conditions from BM to TGM. In addition, under medium-high scanning velocities, the thickness of heated volume may not depend on sheet thickness. Indeed, as shown in Fig. 8(b) if the sample thickness is larger than 0.5 mm, the heated volume is localized within a layer 0.4 mm thick regardless the sample thickness. Therefore, the heated volume thickness, s_1, to take into account cannot depend on the sample thickness in clear contrast with Vollertsen's assumption.

3.2.2 Deformation Field. The variation of final angular distortion with laser source speed under different laser powers and different thicknesses is reported in Fig. 9 for a specimen of AISI 304. A peak of bending angle is shown on sheet sample with smaller thickness. The occurrence of such a peak does not depend on laser power, but rather on sheet thickness. Referring to Fig. 9, the peak of the angular distortion moves towards lower values of scanning velocity as the sheet thickness increases and it is not exhibited on thicker sheets, i.e., s = 1.25 mm and s = 1.50 mm. As previously mentioned, the occurrence of a peak in the angular distortion characterizes the transition from BM to TGM deformation mechanisms. Given a laser beam spot size, the coexistence of BM and TGM deformation mechanisms extends to high values of scanning velocity, i.e., v = 40 mm/s in a sheet of thickness s = 0.75 mm, while an increase of 30% of thickness, i.e., s = 1.0 mm determines a reduction of such transition zone which is reduced to a scanning velocity of 20 mm/s. A further increase of sheet thickness, i.e., s = 1.25 mm and s = 1.50 mm determined the complete disappearing of such transition zone and the trend of bending angle is monotonically descendent with scanning velocity indicating a pure TGM deformation mechanism (Fig. 10).

3.2.3 Application of Proposed Model on High Conductive Materials. An additional campaign of experimental tests was conducted on AA 6013 aluminum alloy to evaluate the model accuracy on such a high conductive material. In this case, the experimental tests were conducted under a scanning speed varying between 10 and 100 mm/s and a laser power

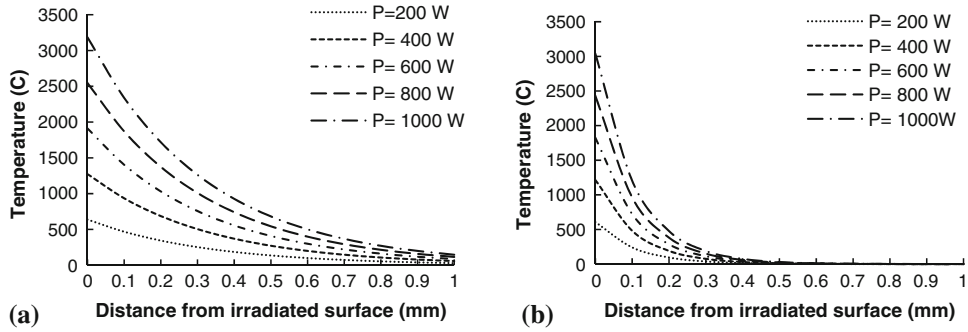

Fig. 9 Temperature distribution as predicted by present model along sheet thickness (s = 1 mm) under different scanning velocities. (a) v = 25 mm/s, (b) v = 75 mm/s and laser powers of AISI 304 material

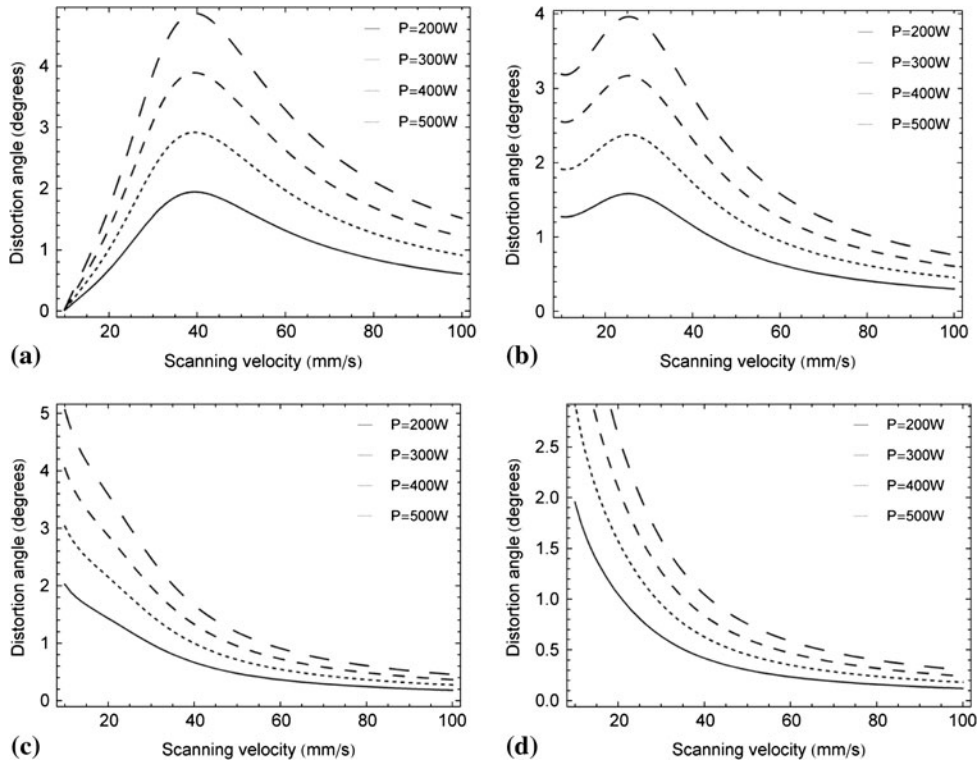

Fig. 10 Variation of the final angular distortion with the laser source speed at different laser powers as predicted by proposed model on samples of AISI 304 with different thicknesses. (a) s = 0.75 mm, (b) s = 1.00 mm, (c) s = 1.25 mm, (d) s = 1.50 mm

between 200 and 1000 W. Thermal properties of AA 6013 are reported in Table 2. The experimental measurements of bending angle, Vollertsen and proposed model predictions are reported in Fig. 11. As can be noted, regardless the processing conditions both models overestimate the bending angle and a very high divergence is shown from models predictions as compared to experimental findings under low scanning speeds and thick samples. Conversely, at higher speeds both models predict the bending angles with higher accuracy the proposed one being closer to experimental measurements. Finally, while Vollertsen model completely fails to predict the bending angles under slow scanning speeds and thin samples as shown in Fig. 11(a) to (c), the proposed model agrees relatively well with experimental measurements. The main cause of this deviation has to be searched on the assumption of neglecting heat conduction towards surrounding material. Indeed, especially under low speed, high power and thick samples, high heat conduction should be included in the calculation on temperature profile along thickness.

4. Conclusions

A closed-form analytical model is developed to evaluate the distortion angle after laser-forming process. A series of experimental tests on AISI 304 stainless steel are conducted by varying the laser power, scanning speed, and sample thickness among several values to investigate the developed model accuracy at very different conditions. In addition, some data reported in literature on a different material (Shipbuilding D36 steel) are also used to evaluate the model accuracy over a

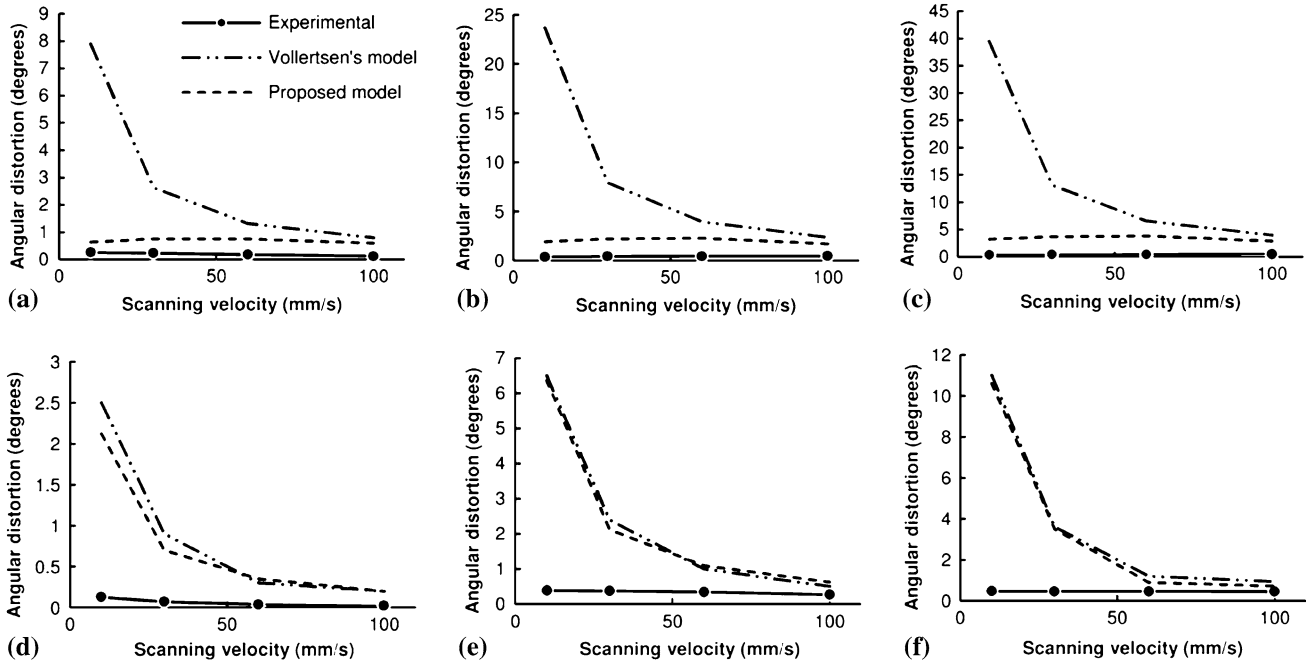

Fig. 11 Experimental measurement and models predictions of angular distortion under different processing conditions on AA 6013 samples: (a) $s = 1$ mm, $P = 200$ W; (b) $s = 1$ mm, $P = 600$ W; (c) $s = 1$ mm, $P = 1000$ W; (d) $s = 2$ mm, $P = 200$ W; (e) $s = 2$ mm, $P = 600$ W; (f) $s = 2$ mm, $P = 1000$ W

wide range of process conditions. The proposed model is capable to evaluate the bending angle under pure TGM conditions and BM to TGM transition conditions. The peak of bending angle versus scanning velocity which was found in literature and experimental tests was effectively predicted by the proposed model. On the other hand, from the test conducted on aluminum alloy, it was demonstrated that, on high conductive materials, the present model is much more accurate than Vollertsen's but its employment is limited to a qualitative estimation of bending angle, such a limit being related to the large amount of heat conduction that the model does not account. Regarding process conditions producing pure TGM deformation mechanism, the model has demonstrated to accurately describe the dependency of final bending angle on both AISI 304 and D36 steels. The beneficial of such a model is represented by the closed formulation which permits to estimate the final bending angle without recurring to numerical integration and therefore the computing time is extremely short.

References

1. H. Shen and F. Vollertsen, Modelling of Laser Forming—An Review, *Comput. Mater. Sci.*, 2009, **46**(4), p 834–840. doi:10.1016/j.commatsci.2009.04.022
2. P. Cheng, Y. Fan, J. Zhang, Y.L. Yao, D.P. Mika, W. Zhang, M. Graham, J. Marte, and M. Jones, Laser Forming of Varying Thickness Plate-Part I: Process Analysis, *J. Manuf. Sci. Eng.*, 2006, **128**(3), p 634. doi:10.1115/1.2172280
3. W. Li and L. Yao, Numerical and Experimental Study of Strain Rate Effects in Laser Forming, *J. Manuf. Sci. Eng.*, 2000, **122**(3), p 445–451. doi:10.1115/1.1286731
4. P. Cheng, Y. Fan, J. Zhang, Y.L. Yao, D.P. Mika, W. Zhang, M. Graham, J. Marte, and M. Jones, Laser Forming of Varying Thickness Plate-Part II: Process Synthesis, *J. Manuf. Sci. Eng.*, 2006, **128**(3), p 642. doi:10.1115/1.2162912
5. F. Vollertsen, An Analytical Model for Laser Bending, *Lasers Eng.*, 1994, **2**, p 261–276
6. M. Hoseinpour Gollo, S.M. Mahdavian, and H. Moslemi Naeini, Statistical Analysis of Parameter Effects on Bending Angle in Laser Forming Process by Pulsed Nd:YAG Laser, *Opt. Laser Technol.*, 2011, **43**(3), p 475–482. doi:10.1016/j.optlastec.2010.07.004
7. P.J. Cheng and S.C. Lin, An Analytical Model for the Temperature Field in the Laser Forming of Sheet Metal, *J. Mater. Process. Technol.*, 2000, **101**, p 260–267
8. H. Shen, Y. Shi, Z. Yao, and J. Hu, An Analytical Model for Estimating Deformation in Laser Forming, *Comput. Mater. Sci.*, 2006, **37**(4), p 593–598. doi:10.1016/j.commatsci.2005.12.030
9. Yau CL, Chan KC, and Lee WB, A New Analytical Model for Laser Bending, *LANE*, 1997. p 357–366
10. H. Shen, Z. Yao, Y. Shi, and J. Hu, An Analytical Formula for Estimating the Bending Angle by Laser Forming, *J. Mech. Eng. Sci.*, 2006, **220**(2), p 243–247
11. L. Zhang, Finite Element Modeling Discretization Requirements for the Laser Forming Process, *Int. J. Mech. Sci.*, 2004, **46**(4), p 623–637. doi:10.1016/j.ijmecsci.2004.04.001
12. P. Zhang, B. Guo, D. Shan, and Z. Ji, FE Simulation of Laser Curve Bending of Sheet Metals, *J. Mater. Process. Technol.*, 2007, **184**(1–3), p 157–162. doi:10.1016/j.jmatprotec.2006.11.017
13. F. Liu, K. Chan, and C. Tang, Numerical Simulation of Laser Forming of Aluminum Matrix Composites with Different Volume Fractions of Reinforcement, *Mater. Sci. Eng. A*, 2007, **458**(1–2), p 48–57. doi:10.1016/j.msea.2006.12.110
14. Z. Ji and S. Wu, FEM Simulation of the Temperature Field During the Laser Forming of Sheet Metal, *J. Mater. Process. Technol.*, 1998, **74**, p 89–95
15. A.K. Kyrsanidi, T.B. Kermanidis, and S.G. Pantelakis, An Analytical Model for the Prediction of Distortions Caused by the Laser Forming Process, *J. Mater. Process. Technol.*, 2000, **104**, p 94–102